4.4.8 Nitrogen-Therminol-Magnetite System

Three single heat transfer probes (19.0, 31.8 and 50.8 mm) axially heated in the 0.108 m dia. bubble column were used to measure heat transfer coefficients. Magnetite powders of three mean sizes (27.7, 36.6 and 45.5 μm) were used in slurry concentrations up to 50 wt%. The h_W data are presented in Fig. 4.40. It is inferred from the data that h_W increases with an increase in U_g and C_s. A plot of the data to highlight the effect of d_p on h_W indicate (Fig. 4.41) that its influence is small. In Fig. 4.42, the h_W values are shown as a function of U_g with tube diameter as parameters. It is noted that h_W decreases with an increase in tube diameter and this decrease is more pronounced with the increase in C_s. The above trends in h_W may be attributed to restricted liquid circulation in highly viscous system in the annulus region between the probes and the column. The h_W data at a given C_s and probe are given in Table 4.22.

4.5 Gas Holdup Data for the Large Column

The experimental gas holdup studies are conducted in the 0.305 m internal diameter bubble column in the semi-batch mode over a temperature range 300-523 K for two- and three-phase systems. The column is equipped with one of the four configurations used for heat transfer surfaces. These are: a 19 mm axially heated single tube , a five-tube , a seven-tube or a thirty-seven tube bundle. The systems studied are air-water, air-water-silica sand, air-water-glass bead, air-water-magnetite, Therminol-nitrogen, and Therminol-nitrogen-magnetite. Powders in the size range (27.7 to 212,0 μm) are used in the slurry concentration range up to 40 wt %. Typical ranges of properties of fluids are given in Table 4.1.

4.5.1 Operating Mode and a Typical Procedure

The average and local gas holdup is measured as a function of gas velocity in the range 1.6 to 37.6 cm/s. Liquid-solid slurry is filled to an initial slumped height (H_{SL}), and the column is expanded up to the maximum gas velocity. The expanded column height (H_e) is recorded and thereafter the gas velocity is

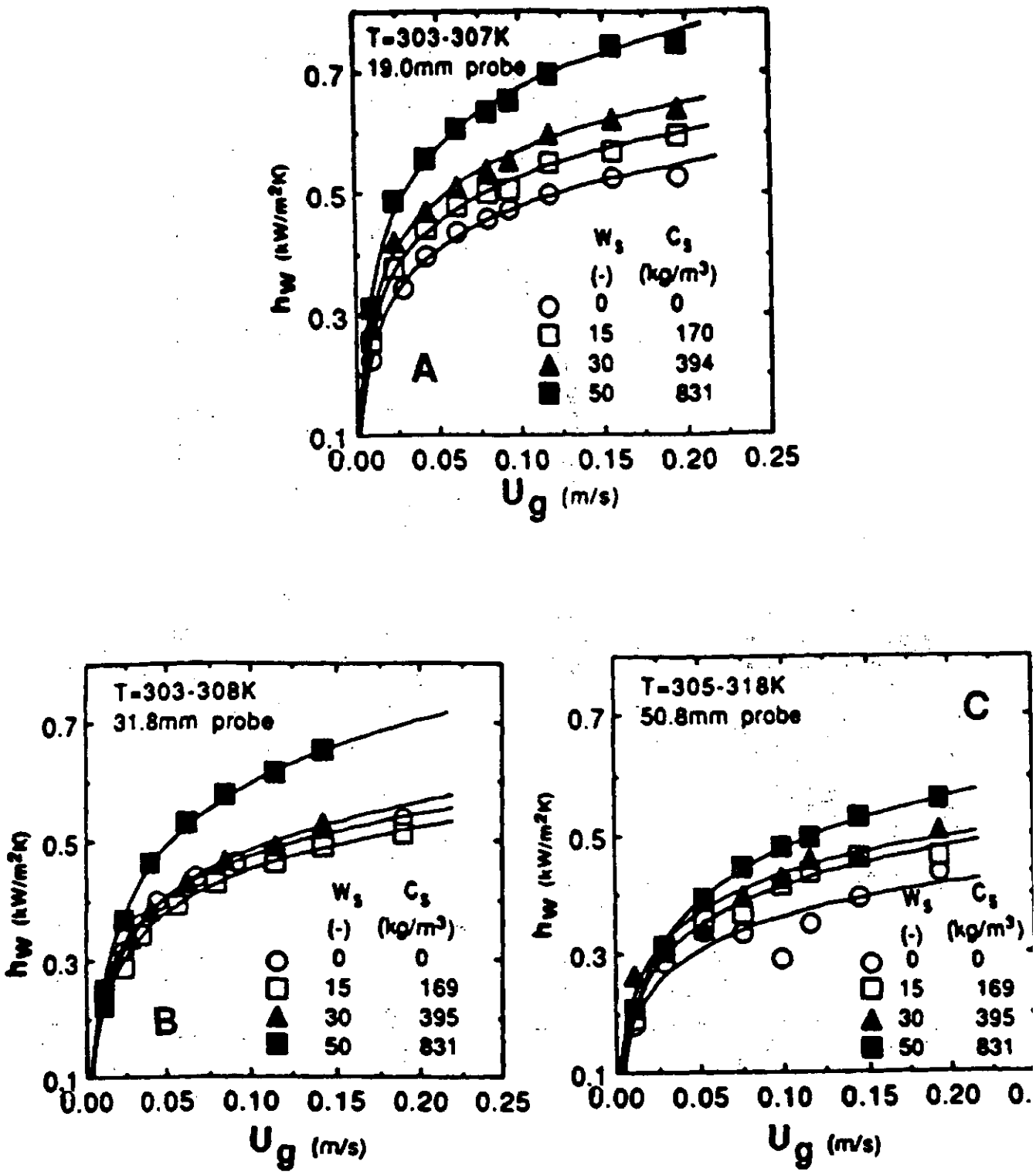

Fig. 4.40. Influence of nitrogen velocity and solids concentration on heat transfer coefficient for the nitrogen-Therminol-magnetite (36.6 μm) system for three probes.

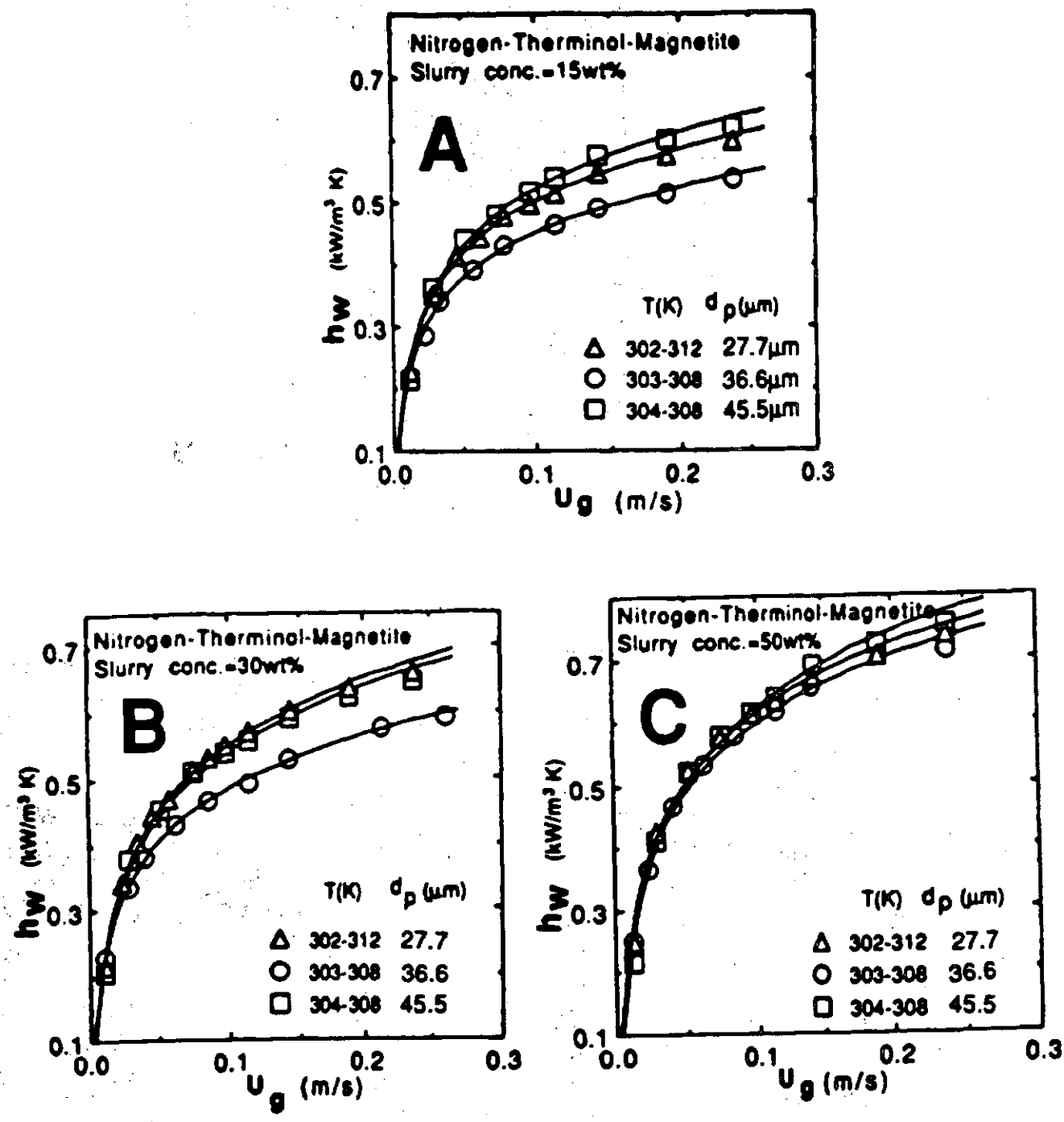

Fig. 4.41. Effect of particle diameter on heat transfer coefficient for the 31.8 mm probe at solids concentrations in weight percent of (A): 15, (B): 30, and (C): 50.

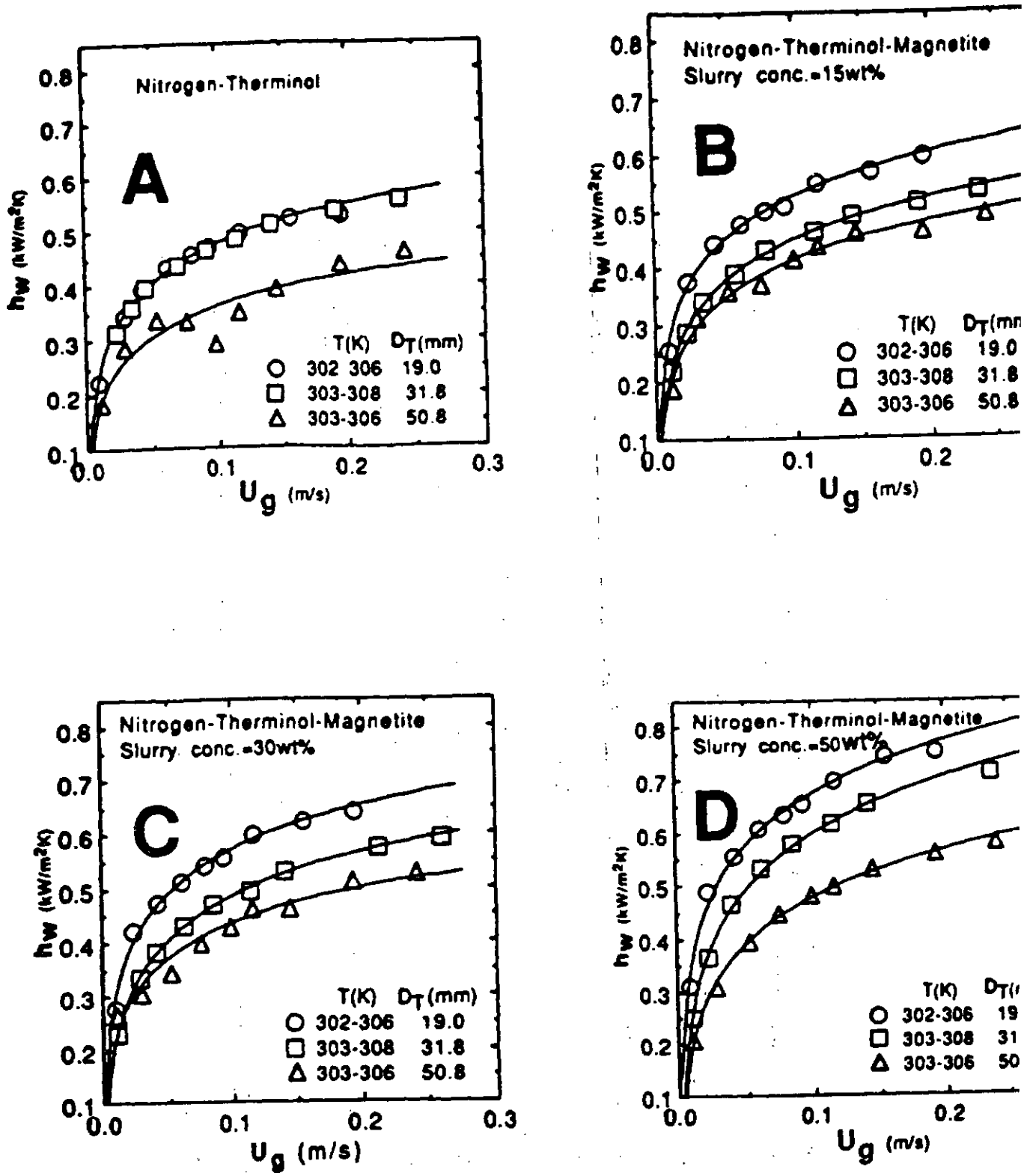

Fig. 4.42. Effect of probe diameter on heat transfer coefficient at different solids concentrations in weight percent of (A): 0, (B): 15, (C): 30, and (D): 50.

Table 4.22. Smothed h_W (kW/m^{2}K) values for nitrogen-Therminol-magnetite system at 306K. Column diameter: 0.108 m, Internal: 19.0, 31.8 and 51.8 mm single tubes, Particle diameters: 26.6, 37.7 and 45.5 μm.

U_g	0%	15%	30%	50%	0%	15%	30%	50%	0%	15%	30%	50%
(m/s)	19.0 mm				31.8 mm				51.8 mm			
0.025	0.340	0.375	0.405	0.470	0.320	0.300	0.320	0.380	0.250	0.282	0.300	0.310
0.050	0.410	0.450	0.490	0.575	0.390	0.380	0.405	0.490	0.310	0.348	0.370	0.385
0.075	0.450	0.495	0.542	0.635	0.430	0.420	0.450	0.550	0.340	0.385	0.408	0.438
0.100	0.480	0.530	0.570	0.675	0.462	0.450	0.488	0.597	0.362	0.412	0.435	0.475
0.125	0.502	0.551	0.595	0.708	0.485	0.478	0.510	0.634	0.380	0.440	0.458	0.510
0.150	0.520	0.572	0.620	0.730	0.502	0.495	0.532	0.660	0.400	0.450	0.475	0.530
0.175	0.540	0.590	0.638	0.751	0.520	0.510	0.550	0.685	0.420	0.470	0.487	0.550
0.200	0.550	0.610	0.653	0.775	0.532	0.525	0.565	0.705	0.430	0.480	0.500	0.568

reduced in steps and the gas-liquid dispersion height is noted in each case. From these measurements, the average gas holdup, ϵ_g (U_g), is computed as a function of air velocity (U_g) from the Eq. (4.7).

As shown in Fig. 3.12 the pressure measuring probes are installed along the column wall at heights of 4, 52.3, 160.5 and 218.9 cm above the air distributor plate. The measurements of pressure drops, ΔP, are taken for two initial heights of the water column, 95 and 140 cm. From these data the local air holdup values for the bottom two sections enclosed between probes located at 4, 52.3, and 160.5 cm are computed using Eq. (4.5).

4.5.2 Air-Water System

Average and local air holdup data are obtained in the 0.305 m diameter column with and without a single 19 mm tube internal as a function of air velocity in the range up to 0.376 m/s at ambient temperature (298 K). Data are taken with tap water and distilled water and the slumped height of water is varied in the range 0.95 to 1.70 m. Some foaming is observed particularly at the top of the dispersion but it is relatively much less than what is observed in the smaller 0.108 m diameter column under similar operating conditions. Similar data are taken with distilled water. Both these sets of data are shown in Fig. 4.43 and these are in good agreement with each other. It is important to note that these air holdup values are consistently larger than the values corresponding to the initial water column height of 1.4 m. This would suggest that the bubble coalescence plays a role and as a result the bubble diameter and hence the air holdup is dependent on the height of the dispersion. The greater the initial column height, the smaller is the holdup.

Also shown in Fig. 4.43 are the values obtained in the smaller column (0.108 m diameter) for the same initial water column height of 0.95 m. It will be seen that the agreement in the values of the air holdup for the two columns is good at lower and higher air velocities. The difference in the middle air velocity range is due to increased foaming in the smaller column. Based on these results it would appear that the bubbling phenomenon and the hydrodynamics of these two

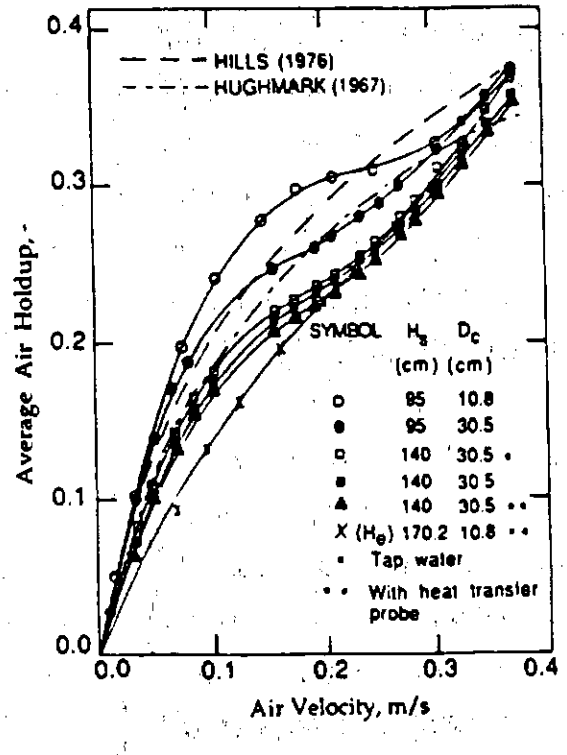

Fig. 4.43. Variation of average air holdup with air velocity and initial water column height.

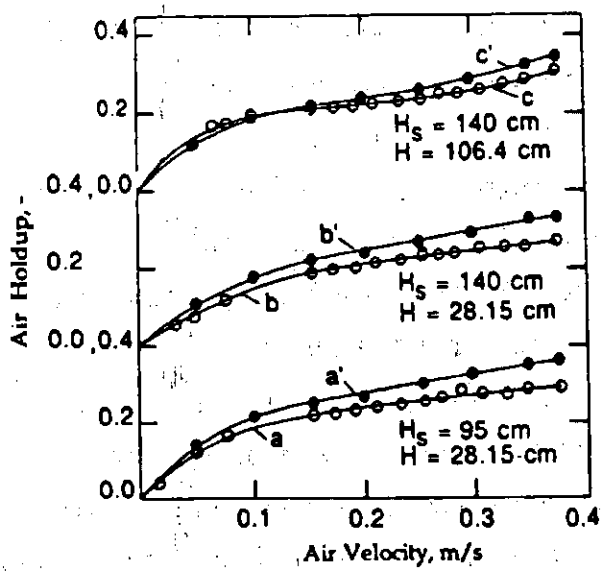

Fig. 4.44. Variation of air holdup in different sections of the larger column with air velocity.

columns is quite similar as long as no foaming occurs. In the smaller column at higher air velocities bumping and bubbles of much larger diameter (slugs) are observed bursting at the column top end. The presence of probe does limit the size of these slugs. Also shown in this figure are the values of the average air holdup as obtained on the two columns with the heat transfer probe present. The two sets of values are in fair agreement with each other and varying values of H_S and the procedure adopted for the case of smaller column is responsible for the difference. Here the air-water dispersion in the small column is always expanded to the overflow position (170.2 cm) so that no foam is encountered. This also explains why this set has smaller values of air holdup than that obtained in the larger column under identical conditions.

These values of the local air holdup are plotted in Fig. 4.44. Curve a refers to the initial water column height of 0.95 m, and represents the air holdup values (local) in the column section enclosed between 4 and 52.3 cm above the distributor plate. The average air holdup values for the entire column as shown in Fig. 4.43 are also displayed as curve *a'*. These values are consistently greater than the local values. This clearly suggests that the local air holdup values are increasing with height in the column.

Curves b and c refer to the initial distilled water column height of 140 cm and for the dispersion sections enclosed between column heights of 4 and 52.3 cm, and 52.3 and 160.5 cm respectively. Curve c represents slightly higher air holdup values than curve b. The average air holdup values (b' and c') are greater than the values of curves b and c for the same air velocity.

Curves b' and c' are identical in magnitude. This clearly suggests that there is a small increase in the air holdup values with increase in height in the column. Increasing bubble coalescence with height in the column as suggested by the results of Fig. 4.43 cannot explain this qualitative dependence of local air holdup on column height and it is attributed to the increased foaming in the column which increase in magnitude with increase in column height and/or to the liquid circulation patterns. Visual observations lend support to this qualitative statement concerning foaming in the column and its variation with height. Similarly liquid circulation is observed as also a variation in its pattern whenever any internal is present.

Air holdup is also measured for decreasing air velocity mode of operation with a 5TB and 7TB internals and the measured values of air holdup for all the three internals (single tube, 1 TB; five tubes, 5TB; and seven tubes, 7TB) are graphed in Fig. 4.45 as a function of air velocity at three temperatures viz., 297, 323 and 343K. The air holdup values at 297K are in good agreement with each other for the five-and seven-tube bundles while these are smaller for the single tube over the entire air velocity range. This can be readily explained on the basis of different bubble coalescence patterns in each case. Bubbles coalesce and grow to a bigger size when only one tube is present and so the air holdup is smaller than for the case of five- or seven- tube bundles where bubbles grow to a relatively smaller size due to the baffling effect of the tubes. Based on the visual observations, the three regimes viz., discrete bubbling, bubble coalescing and coalesced bubble, and their boundaries in terms of air velocity are shown in Fig. 4.45. For the seven-tube bundle, the air holdup decreases as the temperature is increased, and this trend is also confirmed by the two sets of data points for the five-tube bundles is considered adequate at 323K also, as these are at 297K.

A few comments concerning the bubble formation, bubble circulation, and bubble coalescence are in order in relation to the air-holdup data displayed in Figs. 4.44 and 4.45. At room temperature (297K), as the air velocity is increased from zero to 0.04 m/s, uniform bubbles, spherical in shape, are observed throughout the column in increasing number. As the air velocity is further increased up to about 0.06 m/s, the air bubbles descend down near the column wall to be swept up in the inner region of the column and thereby indicating the establishment of a local liquid circulation pattern. This is observed in the upper-half section of the column only. With further increase in the air velocity the liquid circulation pattern descends down in the lower-half section of the column. It is observed up to 0.3 m above the distributor plate at an air velocity of 0.1 m/s. Further, in this air velocity range, the bubble coalescence sets in and 4-5 mm diameter bubbles coalesce to form larger bubbles, about 1 cm in diameter, which rise in the central region of the column along its axis. This bubble dynamic pattern explains the initial increase of air holdup with air velocity and its still rapid increase as the air velocity is increased beyond 0.05 ± 0.01 m/s. As the air velocity is increased beyond 0.1 m/s, the bubble coalescence increases and the size

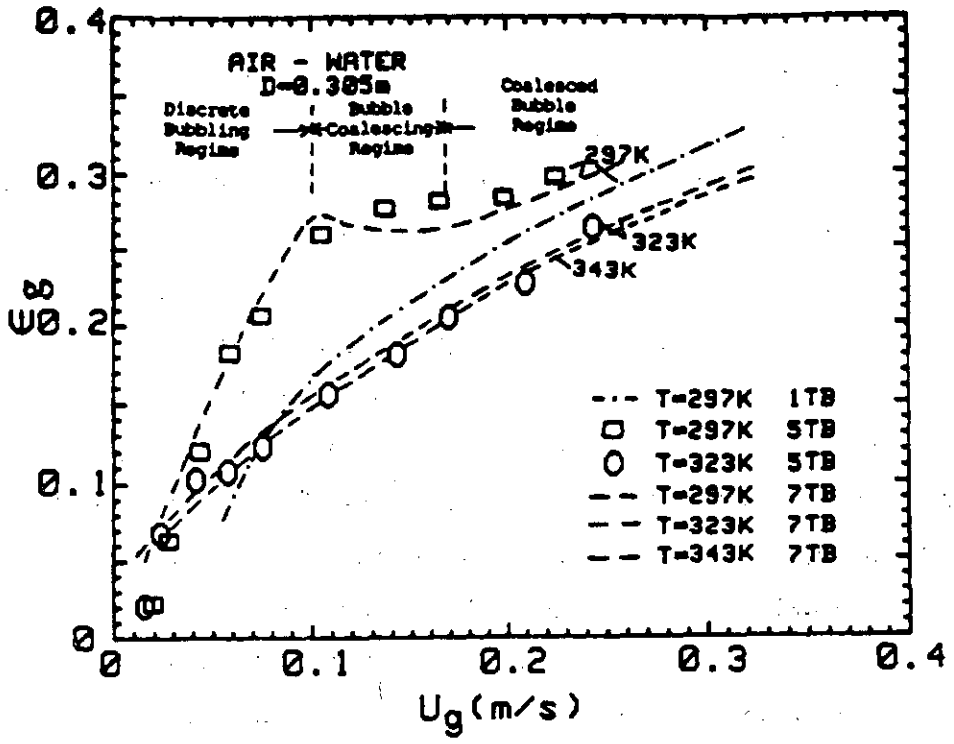

Fig. 4.45. Influence of configuration of internals on air holdup as a function of air velocity and temperature.

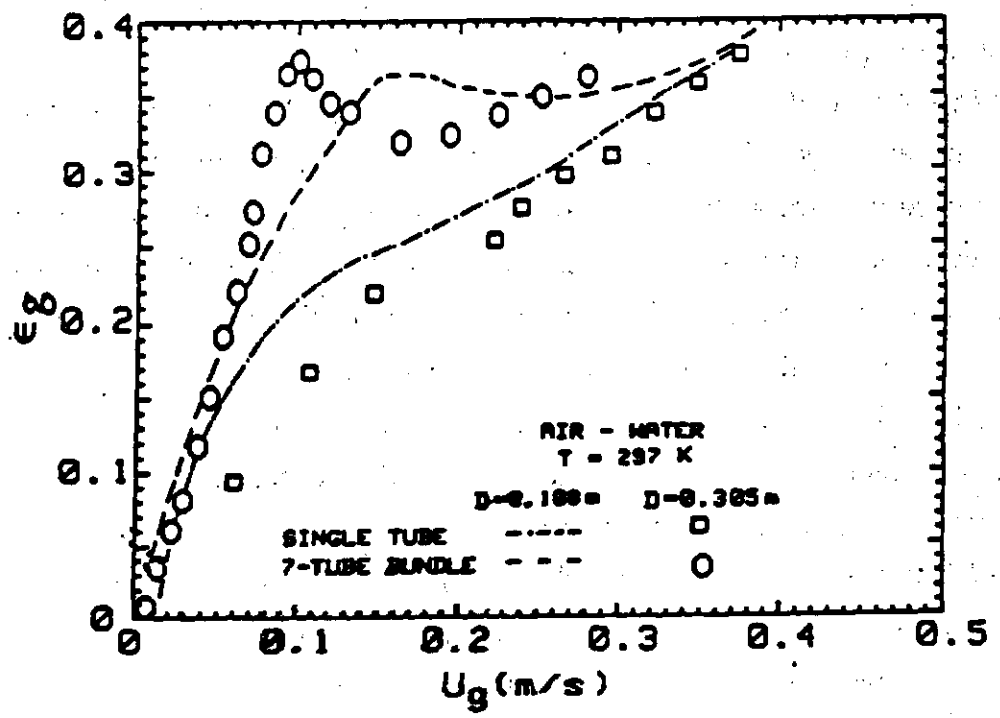

Fig. 4.46. Influence of bubble column diameter and internals on air holdup at 297K as a function of air velocity.

of the coalesced bubbles is up to about 3 cm in diameter. In this bubble coalescing regime, the air holdup decreases with increase in air velocity. The coalesced bubbles assume a maximum stable size at an air velocity of about 0.17 m/s. Further increase in air velocity results only in the increase in the number of coalesced bubbles and hence in the air holdup.

The nature of internals present in the column are primarily responsible for this characteristic variation of air holdup with air velocity. The dashed curve representing the data for the small column with seven-tube bundle in Fig. 4.46 represents similar characteristics variation of air holdup with velocity. On the other hand, both these columns, equipped with only a single tube, produce a different qualitative and quantitative dependence of air holdup on air velocity. Briefly, the coalesced bubbles are much larger for the single tube case so that the gas holdup is smaller than for the seven-tube bundle over the entire air velocity range. A bundle of tubes helps to limit the size of the coalesced bubbles.

As the temperature is increased the region of uniform bubbling shrinks a little bit, the bubble coalescence sets in earlier at an air velocity of about 0.08 m/s and occurs at a relatively rapid rate. The size of coalesced bubbles is larger than at room temperature. This results in an apparent monotonic increase of air holdup with air velocity and a decrease in air holdup with increase in temperature at a given velocity. These qualitative trends decrease in magnitude with further increase in temperature so that the air holdup values exhibit a relatively smaller change as the temperature is increased from 323 to 343K. The air-holdup values are listed in Table 4.23, as functions of air velocity and temperature.

Based on the results displayed in Figs. 4.43, 4.46 and 4.62, and it is clear that the influence of column diameter on air holdup is relatively minor than on the heat transfer coefficient. Botton et al. [124] based on their data for air-water system at room temperature and with columns of diameters 0.020, 0.075, 0.250 and 0.480 m have concluded that the gas holdup increases with the decrease in column diameter as long as its value is less than 0.25 m. The holdup was found to be the same for columns of diameters 0.25 and 0.48 m. For columns of smaller diameters, it is understandable that the gas holdup will increase as the wall effect will increase with decrease in column diameter. An important parameter to

Table 4.23. Air holdup values smoothed over-concentration range for air-water and air-water-glass bead systems for different particle diameters and at different temperature levels. Column diameter: 0.305 m, Internal: Seven-tube bundle.

U_g	Solids conc. = 0 wt.%				Solids conc. = 5-20 wt% (d_p = 143.3 μm)			Solids conc. = 5 wt.% (d_p = 90 μm)			Solids conc. = 5 wt.% (d_p = 50 μm)		
(m/s)	297K	313K	323K	343K	297K	323K	343K	297K	323K	343K	297K	323K	343K
0.02	0.050	0.052	0.042	0.043	0.058	0.035	0.040	0.031	0.029	0.029	0.065	---	---
0.03	0.080	0.086	0.055	0.053	0.088	0.045	0.060	0.051	0.042	0.042	0.084	0.050	0.058
0.05	0.170	0.125	0.100	0.083	0.150	0.078	0.095	0.085	0.069	0.069	0.115	0.082	0.082
0.07	0.245	0.172	0.121	0.102	0.210	0.100	0.120	0.110	0.098	0.098	0.138	0.110	0.110
0.10	0.370	0.202	0.155	0.153	0.270	0.133	0.152	0.140	0.129	0.129	0.170	0.148	0.150
0.15	0.321	0.264	0.182	0.180	0.270	0.170	0.180	0.185	0.175	0.175	0.210	0.190	0.200
0.20	0.322	0.322	0.236	0.234	0.278	0.212	0.245	0.220	0.205	0.205	0.248	0.228	0.238
0.22	0.336	0.336	0.240	0.240	0.290	0.222	0.260	0.235	0.221	0.221	0.262	0.244	0.250
0.24	0.345	0.350	0.256	0.256	0.310	0.290	0.270	0.231	0.241	0.241	---	0.258	0.263
0.26	0.350	---	0.372	0.372	---	---	0.280	---	---	---	---	---	0.276

consider would be the equivalent diameter for fluid flow defined as four times the hydraulic radius. The latter is defined as the ratio of the column cross-sectional area available for fluid flow to the wetted perimeter. For the cylindrical column geometry and cylindrical axial probe, the equivalent diameter is numerically equal to the difference in the inside column diameter and outside probe diameter. These values are 0.089 and 0.286 m for the smaller and larger column respectively. Our present experimental results suggest that the gas holdup is independent of hydraulic radius in the range (0.022 - 0.072 m) as long as there is no foamy flow regime.

Air holdup is also measured for air-water system with decreasing air velocities at four temperatures (298, 323, 343 and 353K) in larger bubble column equipped with thirty-seven tube bundle. Figure 4.47 shows the variation of air holdup measurements including repeated runs as a function of air superficial velocity at different temperatures. The air holdup is found to increase with air velocity. The air holdup dependence on temperature is highlighted in Fig. 4.48. It is to be noted that the air holdup decreases as the temperature is raised above the ambient (298K) and thereafter almost remains constant over the velocity range. The smoothed air holdup data at each temperature is given in Table 4.24 as a function of U_g.

4.5.3 Nitrogen-Therminol System

The nitrogen gas holdup data are measured in the 0.305 m diameter column equipped with thirty-seven bundle in the temperature range 296 to 523K and gas velocity range 0.0015 to 0.139 m/s. The initial liquid slumped heights are varied between 1.4 to 1.6 m. During the star-up the temperature of the liquid is raised to the desired level by energizing four 4kW AC calrod heaters. A temperature controller with a thermocouple feed-back is used to regulate the power supply to the AC heaters and the temperature of the column is maintained within $\pm$ 1°C.

Gas holdup data for both increasing and decreasing gas velocity modes at three temperature levels, is shown in Fig. 4.49A. In both cases, the holdup data are found identical. A similar plot for gas holdup at six temperature levels and for decreasing gas velocity mode is shown later in Fig. 4.59A. The smoothed

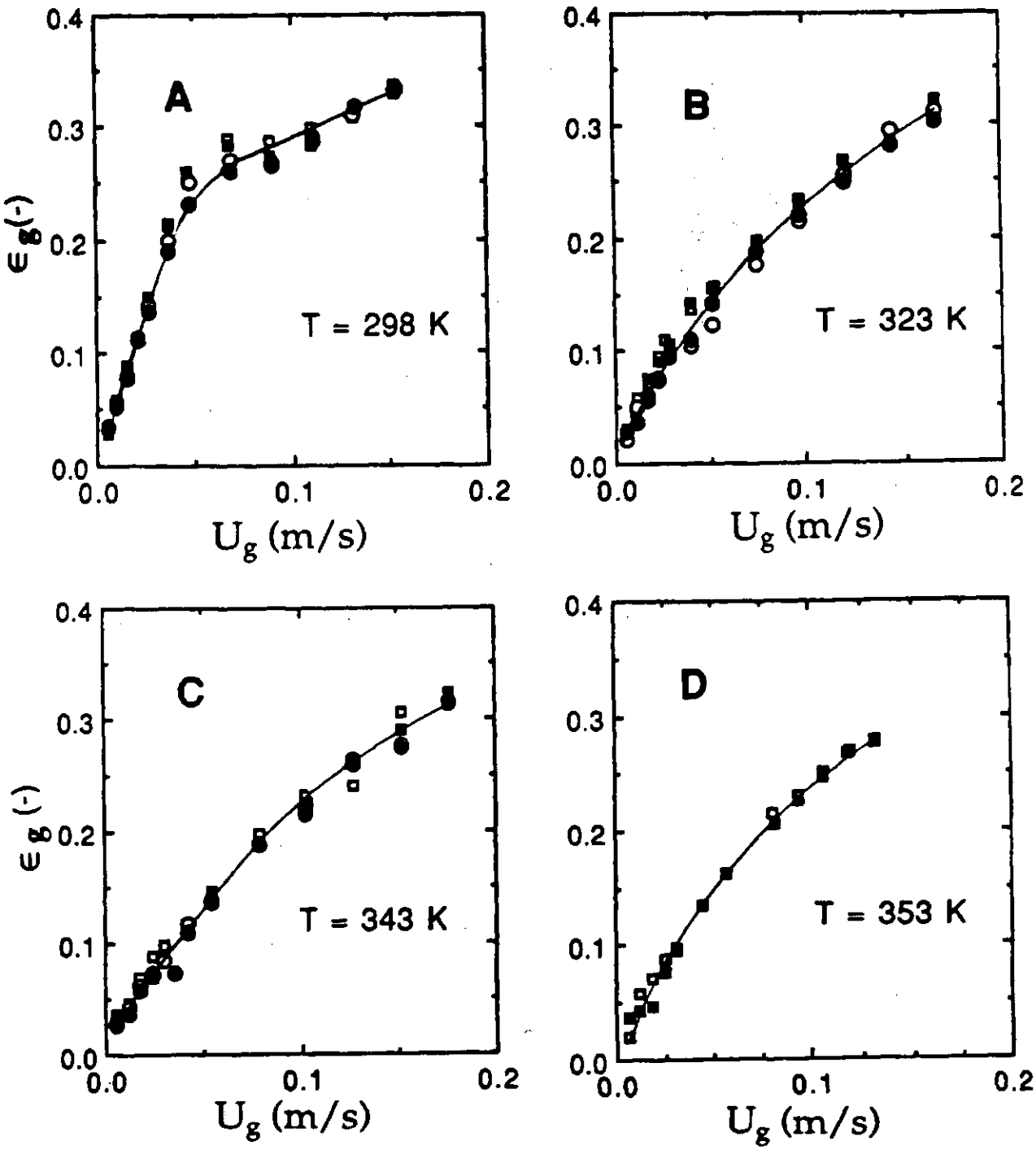

Fig. 4.47. Variation of air holdup with decreasing superficial air velocity for the air-water system at four temperatures. □ SET 1, ■ SET 2, ○ SET 3, • SET 4.

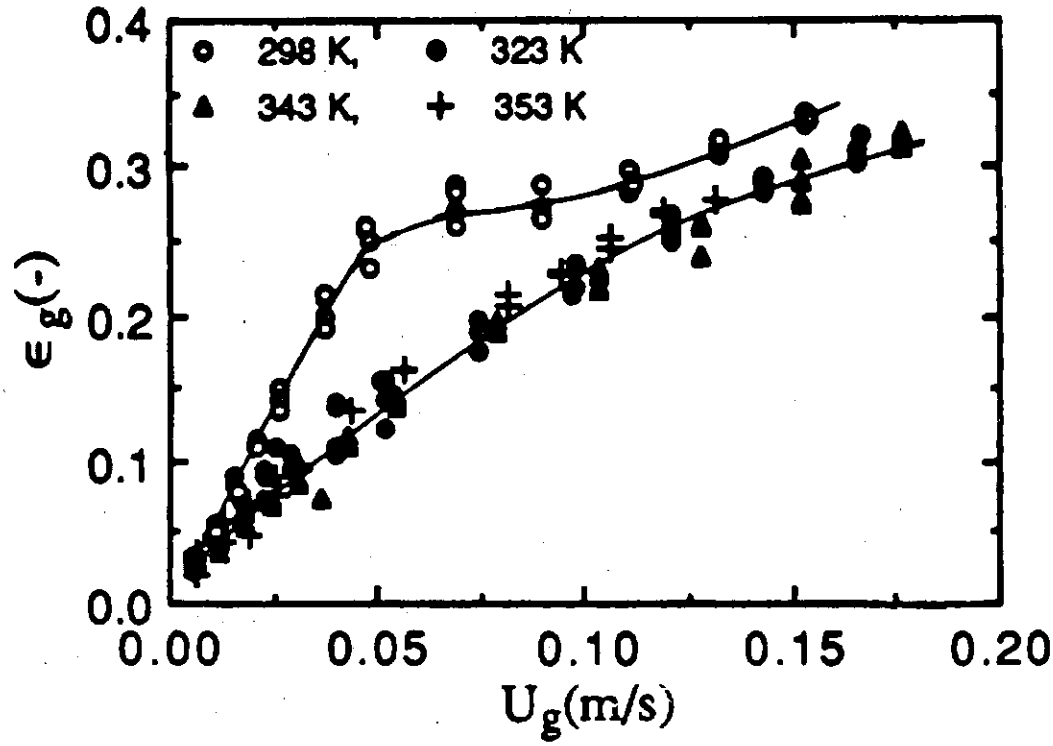

Fig. 4.48. Dependence of air holdup on air velocity and temperature for the column with thirty-seven tube bundle and air-water system.

Table 4.24. Smoothed air holdup values for air-water system at different temperature levels. Column diameter: 0.305 m, Internal: Thirty-seven bundle.

U_g	air holdup			
(m/s)	298K	323K	343K	353K
0.01	0.06	0.04	0.04	0.04
0.02	0.115	0.070	0.068	0.070
0.04	0.220	0.130	0.110	0.123
0.06	0.270	0.160	0.150	0.168
0.08	0.280	0.195	0.190	0.210
0.10	0.280	0.230	0.220	0.240
0.12	0.295	0.255	0.245	0.270
0.14	0.318	0.300	0.275	—
0.16	—	0.310	0.300	—
0.18	—	—	0.320	—

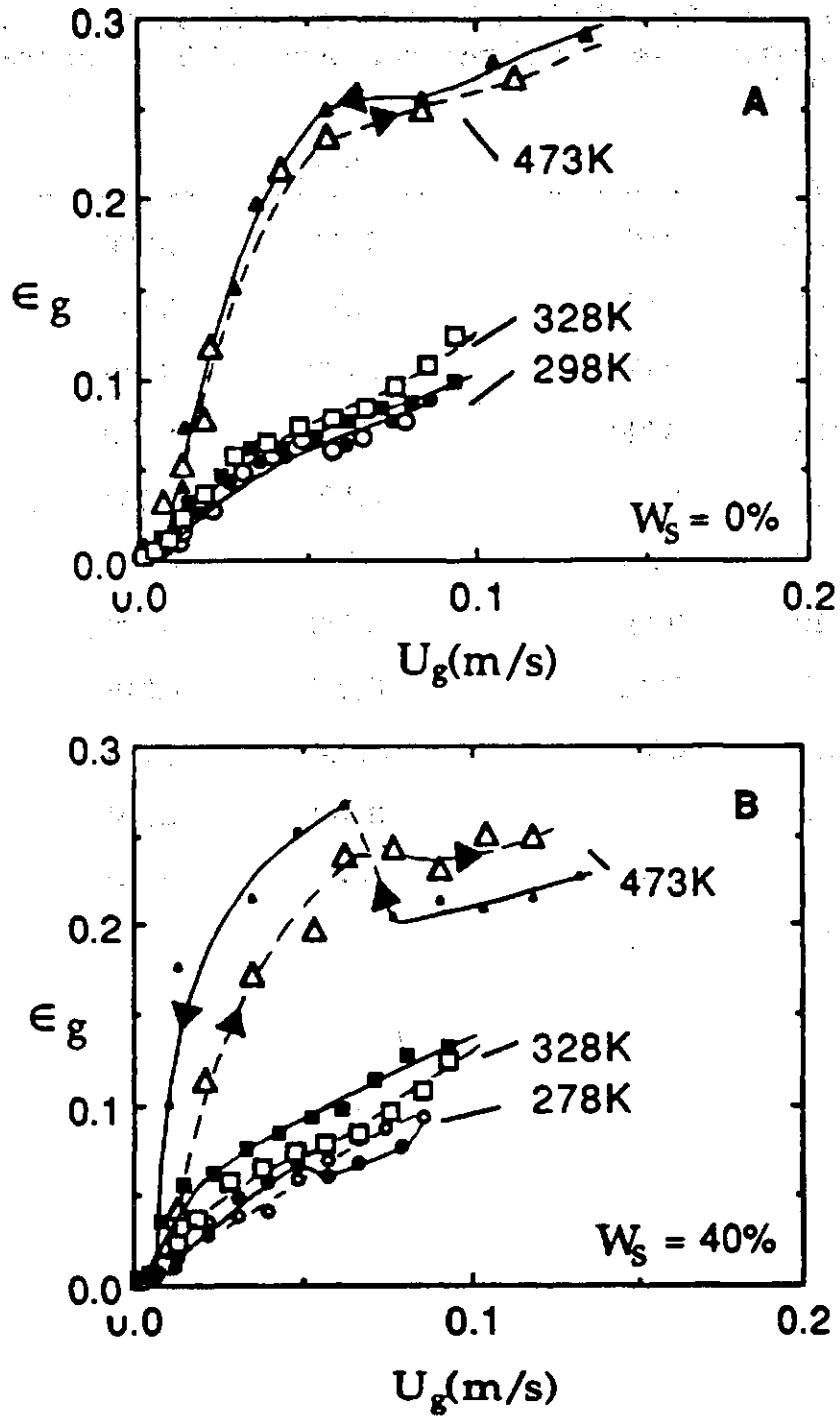

Fig. 4.49. Variation of nitrogen holdup with increasing (○ , □ , △) and decreasing (● , ■ , ▲) velocity at different temperatures and solids concen-trations.

holdup values for decreasing nitrogen gas velocities are given in Table 4.25.

Foaming is observed and in calculating the holdup it is accounted in the dispersion height. The gas holdup increases with increase in nitrogen gas velocity, the rate of increase is dependent on gas velocity and on temperature. At a given nitrogen velocity the holdup decreases slightly as the temperature is raised from ambient 296K to 309K, but then increases as the temperature is raised to 428K, and remains unchanged as the temperature is raised further to 523K. This characteristic dependence of holdup on gas velocity and temperature are to be understood on the basis of changing flow regimes which are encountered at a given temperature level as the gas velocity is decreased. Our visual observations in this connection are detailed below.

For velocities greater than 0.05 m/s and for temperatures in the range 428 - 523K, a large number of relatively smaller bubbles (2 - 5 mm in diameter) are observed throughout the column. Bubble coalescence is observed in the central region of the column, and coalesced bubbles as large as 3 -4 cm diameter emerged from the liquid surface. These bubbles churn the liquid vigorously. Foam is also observed but it is mostly distributed in the dispersion and only a small amount, about 3 - 4 cm in height, accumulates and is distinctly seen at the top of the liquid column. As the velocity is further reduced below 5 cm/s, more and more foam accumulates at the top of the liquid column. However, as the gas velocity is reduced below 3 cm/s, the foam formation decreases, and almost disappears for velocities around 1 cm/s and smaller. At 378K, the same qualitative behavior is observed except the foam formation is much reduced. At lower temperatures (296 and 309K) no foam is observed and bubble coalescence is more pronounced than at higher temperatures. At higher temperatures (378 - 523K) the bubbles formed at the distributor (5 - 7 mm) split into smaller bubbles as they move up in the column. At lower temperatures, smaller than 378K, bubble splitting is not observed and instead bubble coalescence predominates. This general behavior is consistent with the changing viscosity of Therminol with temperature. As the temperature increases, viscosity decreases appreciably and hence smaller bubbles and reduced coalescence give rise to much higher holdup values than those at lower temperatures where the viscosity is relatively large and the bubble size is comparatively larger as also the bubble coalescence. This explains the

Table 4.25. Nitrogen gas holdup values smoothed over the solids concentration range for nitrogen-Therminol-magneti system at different temperature levels. Column diameter: 0.305 m, Internal: Thirty-seven tube bundle, Particle diamet 36.0 μm, solids conc. : 0, 15, 30 and 40 wt%.

U_g	T= 298 K				T= 328 K		T= 378 K	T= 428 K		T= 473 K		T= 523 K	
(m/s)	w_s=0%	15%	30%	40%	0-30%	40%	0-40%	0-30%	40%	0-30%	40%	0%	40%
0.01	0.023	0.012	0.001	0.014	0.022	0.040	0.040	0.050	0.035	—	—	0.040	0.040
0.02	0.040	0.020	0.003	0.030	0.045	0.055	0.085	0.110	0.090	0.120	0.12	0.100	0.080
0.03	0.058	0.028	0.006	0.042	0.058	0.070	0.125	0.160	0.135	0.185	0.18	0.180	0.120
0.04	0.071	0.039	0.010	0.055	0.072	0.082	0.160	0.220	0.170	0.190	0.19	0.200	0.150
0.05	0.085	0.049	0.018	0.065	0.082	0.092	0.180	0.240	0.200	0.260	0.25	0.235	0.170
0.06	0.098	0.060	0.028	0.075	0.090	0.105	0.190	0.250	0.220	0.270	0.25	0.250	0.175
0.07	0.110	0.070	0.040	0.082	0.100	0.104	0.198	0.260	0.230	0.270	0.24	0.255	0.170
0.08	0.120	0.080	0.055	0.090	0.110	0.125	0.200	0.280	0.240	0.280	0.22	0.260	0.175
0.09	0.130	—	—	—	0.110	0.132	0.210	0.281	0.240	0.270	0.21	0.265	0.180
0.10	0.140	—	—	—	0.120	0.140	0.210	0.278	0.245	0.280	0.21	0.270	0.190
0.11	0.150	—	—	—	—	—	0.220	0.280	0.250	0.280	0.21	0.270	0.200
0.12	—	—	—	—	—	—	—	—	0.260	0.270	0.22	0.275	0.210
0.13	—	—	—	—	—	—	—	—	—	0.280	0.23	0.280	0.220
0.14	—	—	—	—	—	—	—	—	—	0.280	—	0.280	0.230

characteristic variation of holdup observed in Fig. 4.49A.

4.5.4 Air-Water-Silica Sand System

The air holdup values for the air-water-sand system are displayed in Fig. 4.50 as a function of air velocity for two slurry concentrations (5 and 10 weight percent) and in each case at three temperatures. The data for air-water system are also shown for comparison. Several interesting conclusions are obvious. The influence of slurry concentration on gas holdup is negligibly small but is most pronounced in the discrete bubbling regime. The influence of temperature in the range (297 - 343K) is small and has the same qualitative decreasing trend with increasing temperature at a given air velocity as observed for the two-phase (gas-liquid) system. These trends are small and their magnitudes are comparable to experimental uncertainties and hence the same are not uniquely obvious. Smoothed air holdup values for the air-water-sand system are listed in Table 4.26.

4.5.5 Air-Water-Glass Bead System

The values of air holdup for a 143.3 μm average diameter slurry of glass beads in water for solids concentrations of 5, 10 and 20 weight percent, as a function of air velocity at temperatures of 297, 323 and 343K, are shown in Fig. 4.51. The presence of solids at 297K reduces the air holdup considerably, except when its concentration is small. With an increase in temperature above 297K, the variation of air holdup for this three-phase system with temperature above 297K and for the solids concentrations investigated here is almost negligibly small. In Table 4.23, are reported these concentration averaged air-holdup values at each of the three temperatures as a function of air velocity. In Fig. 4.52 similar data are presented for 90 and 50 μm average diameter glass bead slurries for the solids concentration of five weight percent. It is seen that at all temperatures the air holdup variation monotonically increases with air velocity and is not much different from the corresponding two-phase air-water system other than at 297K.

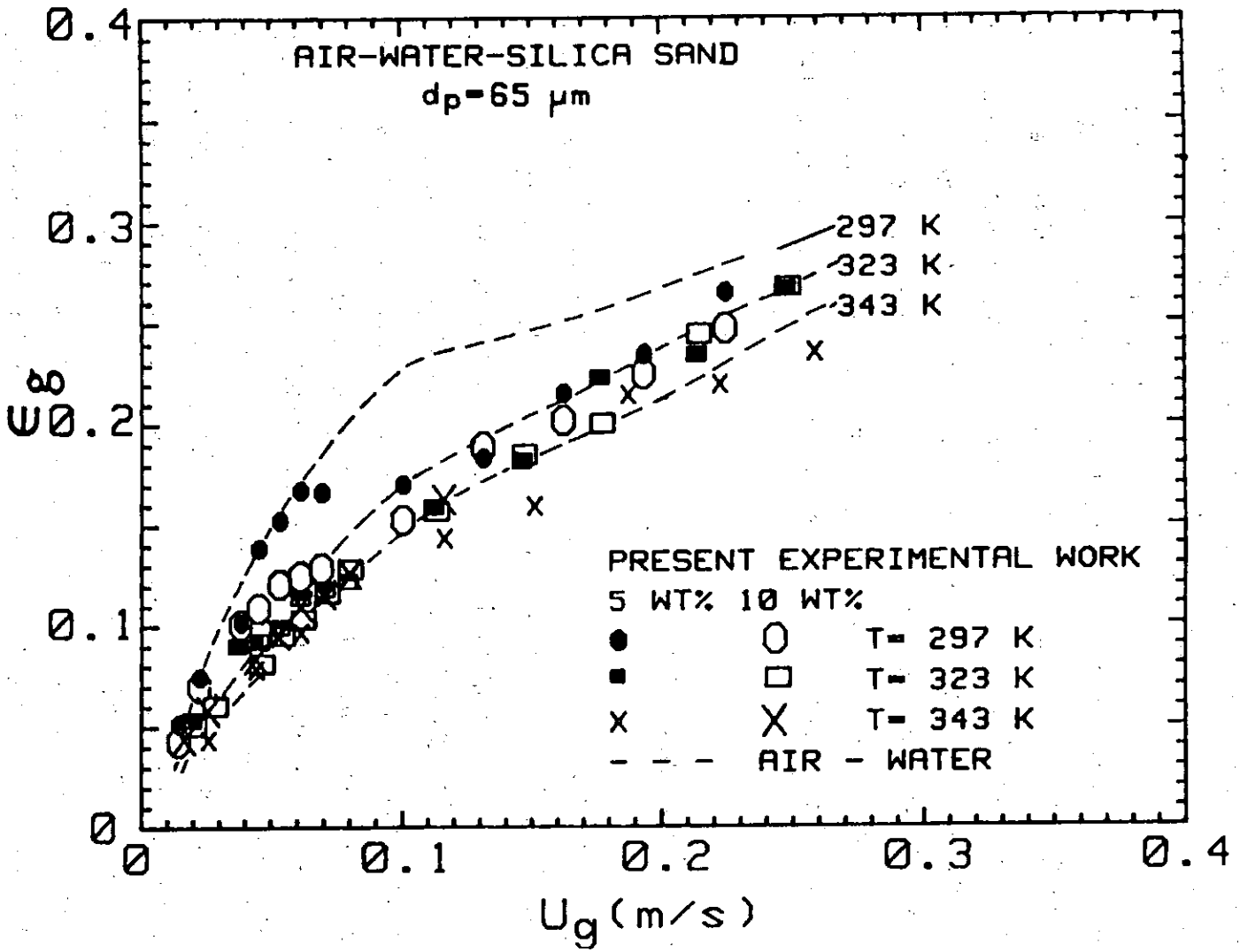

Fig. 4.50. Dependence of air holdup on air velocity, temperature and slurry concentration.

Table 4.26. Smoothed air holdup values for air-water-silica sand system at different temperature levels. Column diameter: 0.305m, Internal: Seven-tube bundle.

U_g (m/s)	Air holdup, ϵ_g (-)					
	Solids conc. = 5 wt% (d_p = 65 μm)			Solids conc. = 10 wt % (d_p = 65 μm)		
	297K	323K	343K	297K	323K	343K
0.02	0.057	0.051	0.050	0.056	0.053	0.050
0.03	0.087	0.075	0.670	0.082	0.067	0.070
0.05	0.151	0.095	0.098	0.121	0.096	0.095
0.07	0.170	0.118	0.120	0.130	0.115	0.118
0.10	0.172	0.144	0.142	0.150	0.140	0.140
0.15	0.198	0.190	0.182	0.196	0.186	0.185
0.20	0.235	0.230	0.228	0.230	0.232	0.230
0.22	0.255	0.250	0.228	0.242	0.246	0.230
0.25	-	0.267	0.248	-	0.269	0.255
0.27	-	-	-	-	-	-

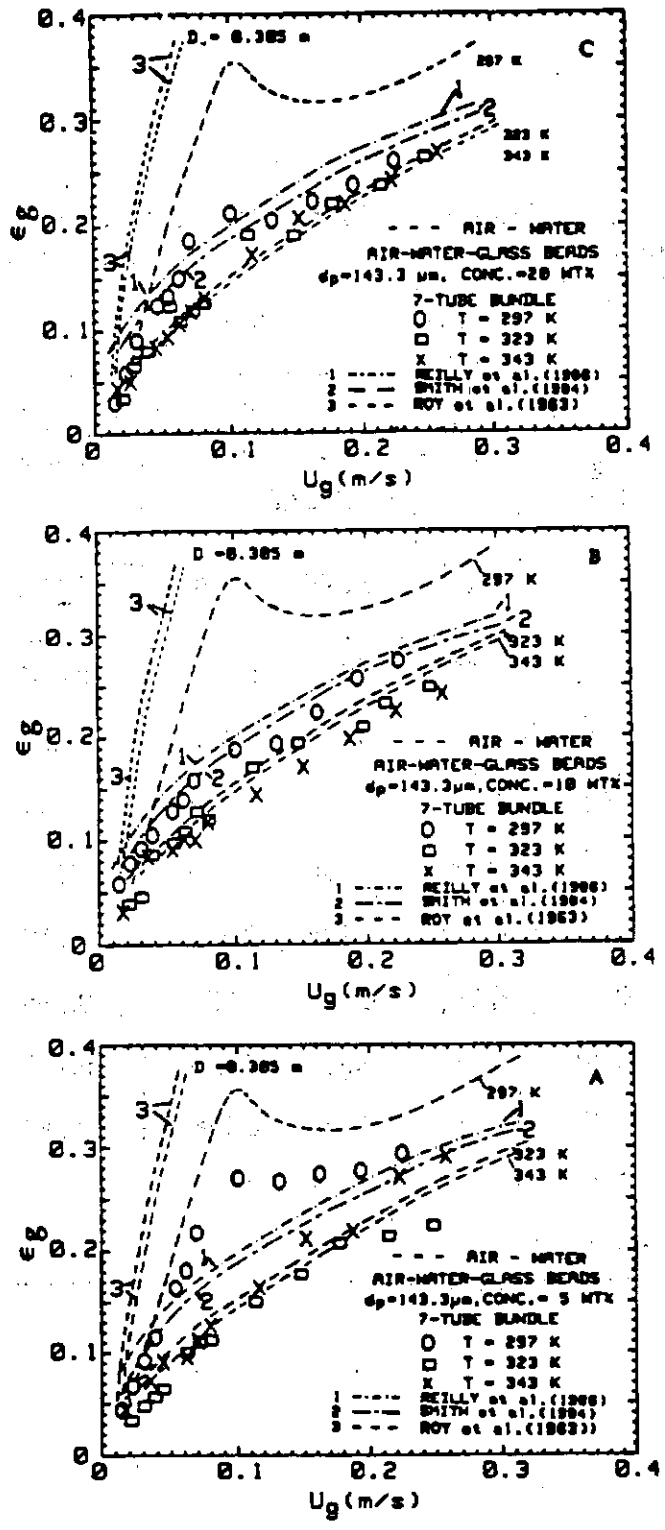

Fig. 4.51. Dependence of air holdup as a function of air velocity and temperature on solids concentration, and its comparison with the predictions of different correlations. The concentrations of glass beads (d_p = 14.3 μm) in the slurry is (A) five (52 kg/m^3), (B) ten (110 kg/m^3), and (C) twenty (249K kg/m^3) weight percent.

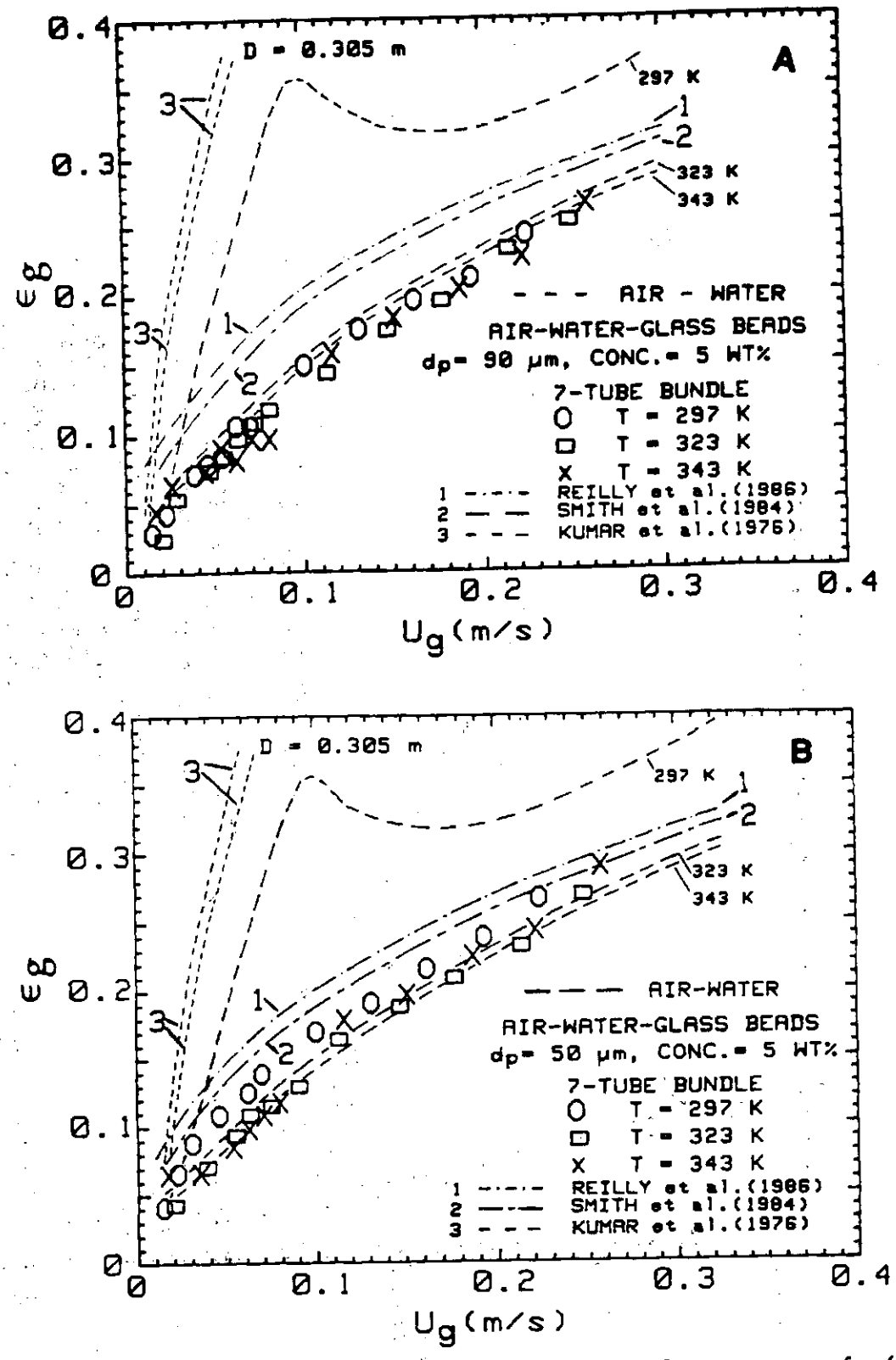

Fig. 4.52. Dependence of air holdup on air velocity and temperature for (A) 90 μm, (B) 50 μm, and (C) 50-90 μm, average size powders. Experimental data are also compared with the predictions of different correlations.

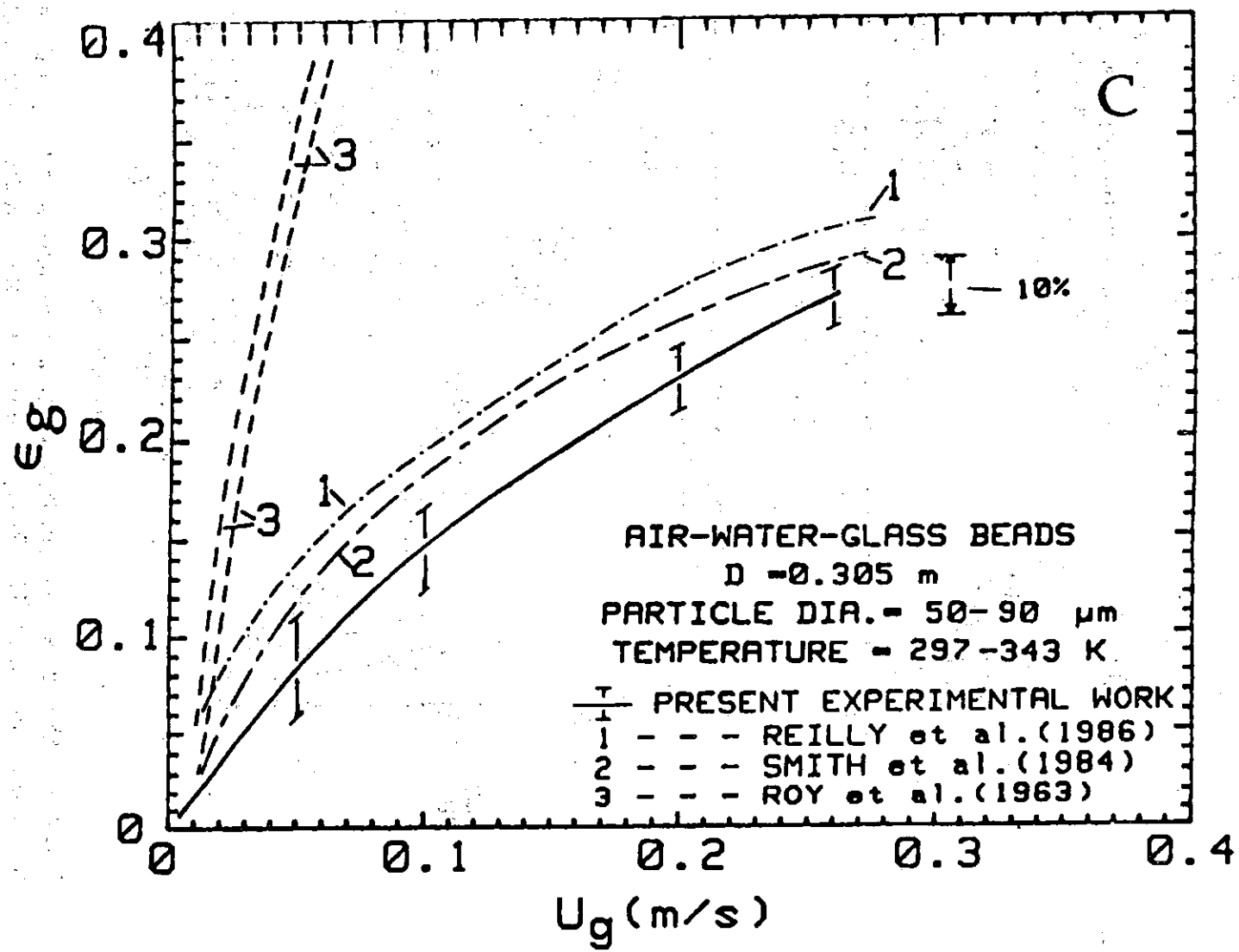

Fig. 4.52. Dependence of air holdup on air velocity and temperature for (A) 90 μm, (B) 50 μm, and (C) 50-90 μm, average size powders. Experimental data are also compared with the predictions of different correlations.

These qualitative features highlight the probable effect of particle diameter on slurry viscosity as further compounded with the influence of temperature. It appears that the bubble-dynamic pattern for systems of particles greater than 100 μm, at room temperature is different than those involving particles smaller than 100 μm, gas holdup has been measured in the large column fitted with a simulated thirty-seven tube bundle for air-water system. Glass beads of three different average diameters have been used. The values are 125 μm, 168 μm and 212 μm. The measurements are taken at three temperatures viz., 298, 323, and 353K. The concentrations of smallest and largest size particles in the slurry are 5 and 15 percent by weight, while it is 30 weight percent for 168 μm size powder. The superficial air velocity is varied up to a maximum value of about 18 cm/s. Discussion of these data is presented in terms of the nature of their variation with air velocity, temperature, particle size in the slurry, and slurry concentration.

Experimental gas holdup results measured in the decreasing superficial air velocity mode at three temperatures (298, 323, and 353K) are reported in Figs. 4.53 to 4.57. The holdup increases with increase in air velocity at each temperature. However, the temperature dependence of air holdup is somewhat involved. The air holdup decreases as the temperature is raised above the ambient (298K). On the other hand for temperatures in the range 323 - 353K, no clear trend could be established on the basis of experimental data. In fact repeated sets of data at the same temperature exhibit scatter of the same magnitude as the variation in the entire temperature range. For slurries of 125 μm and 212 μm particles, two slurry concentrations have been examined, 5 and 15 weight percent. Figure 4.55 presents the single data set for the slurry of 168 μm particles taken for the slurry concentration of 30 weight percent. The holdup in all cases increase with increase in air velocity. The influence of temperature is relatively modest for a given slurry at a given air velocity. However, a small trend in the data suggests that this influence is relatively more for slurries of smaller particles and at smaller concentrations of solids in the slurry of the same particle size. The temperature dependence is pronounced as the temperature is raised above the ambient (298K) but this dependence disappears as the temperature is raised (323 and 353K). For design purposes, it would appear to be appropriate to ignore the

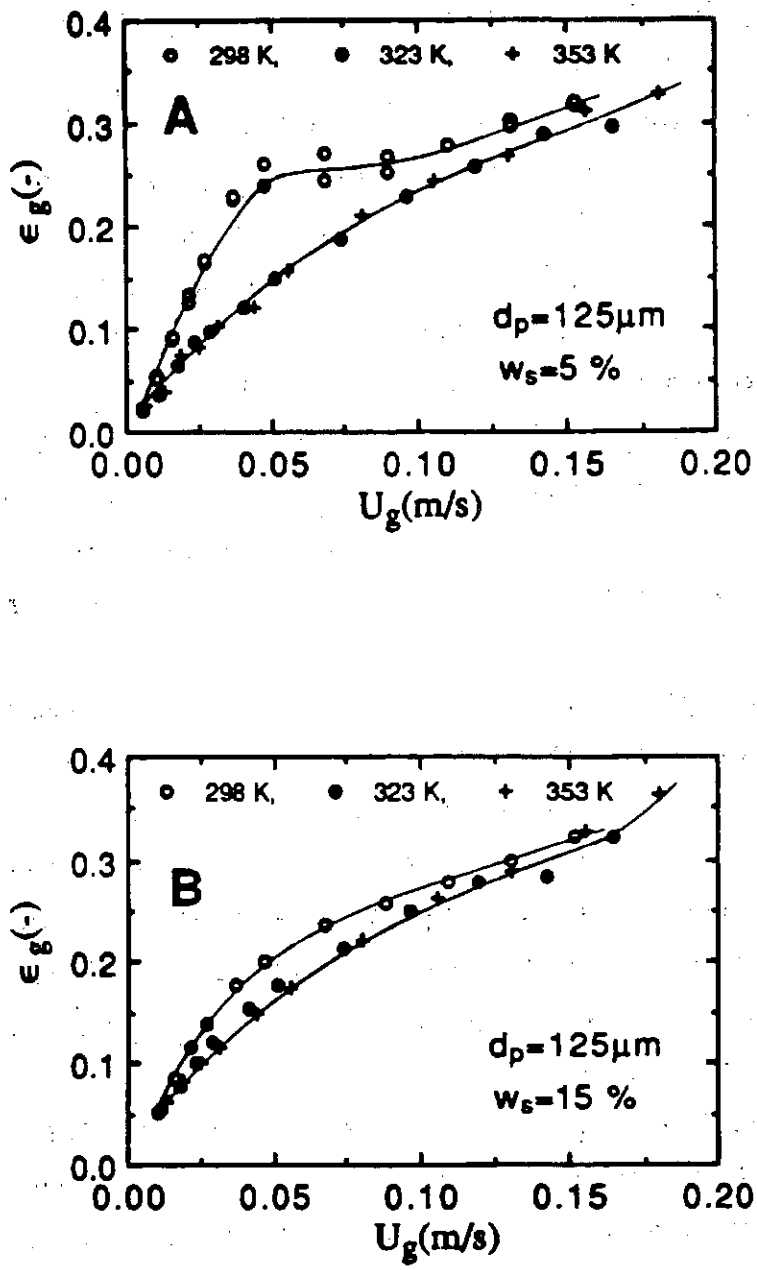

Fig. 4.53. Variation of air holdup for the air-water-glass bead system with decreasing superficial air velocity and temperature for slurries of 125 μm particles at two concentrations.

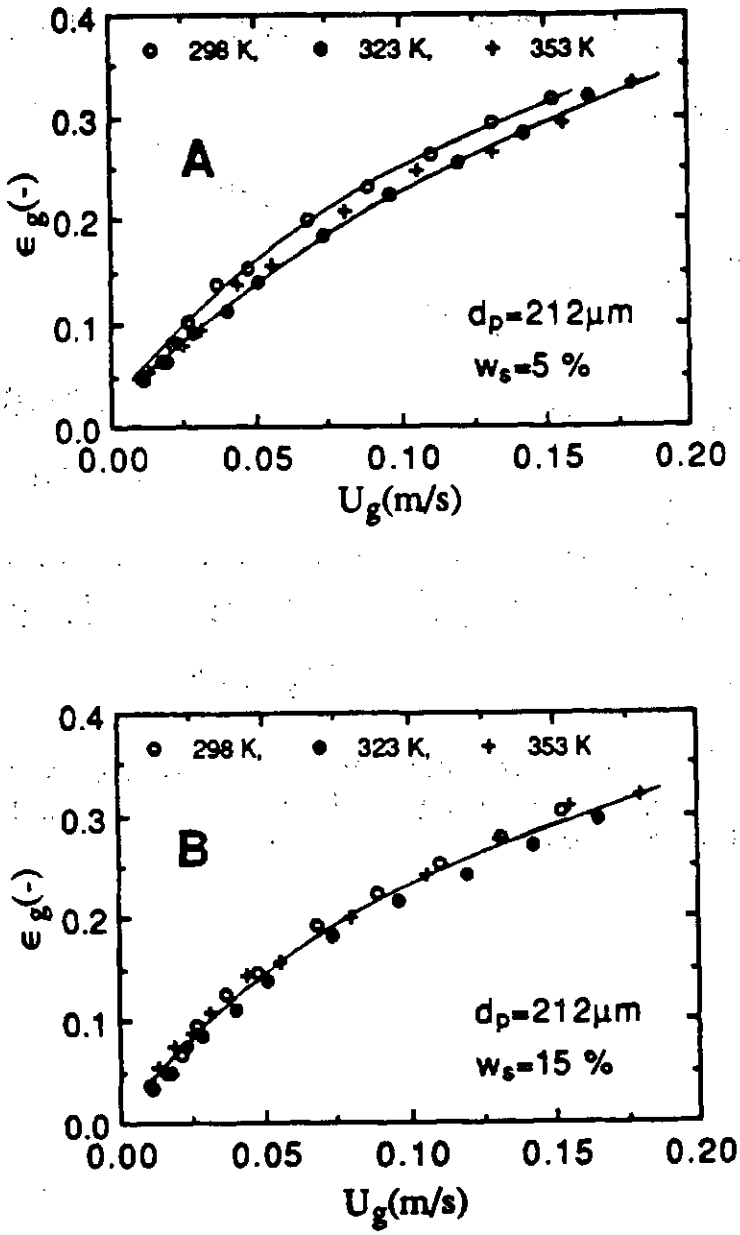

Fig. 4.54. Variation of air holdup for the air-water-glass bead system with decreasing superficial air velocity and temperature for slurries of 212 μm particles at two concentrations.

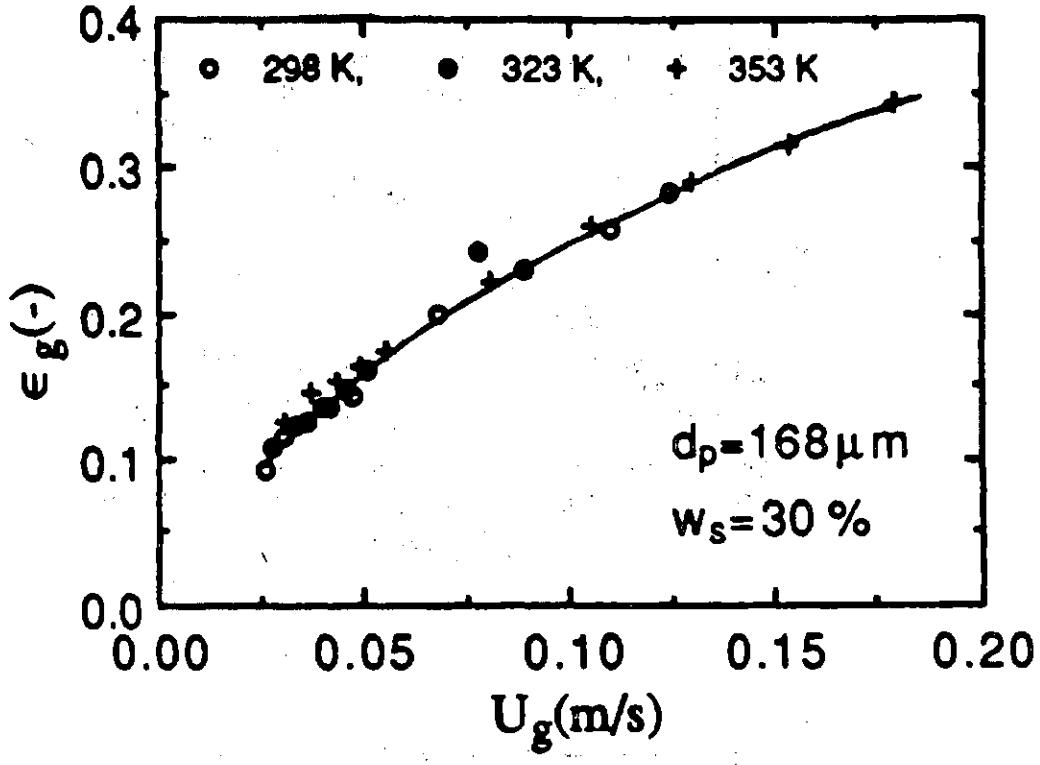

Fig. 4.55. Variation of air holdup for the air-water-glass bead system with decreasing superficial air velocity and temperature for the large column with thirty-seven tube bundle.

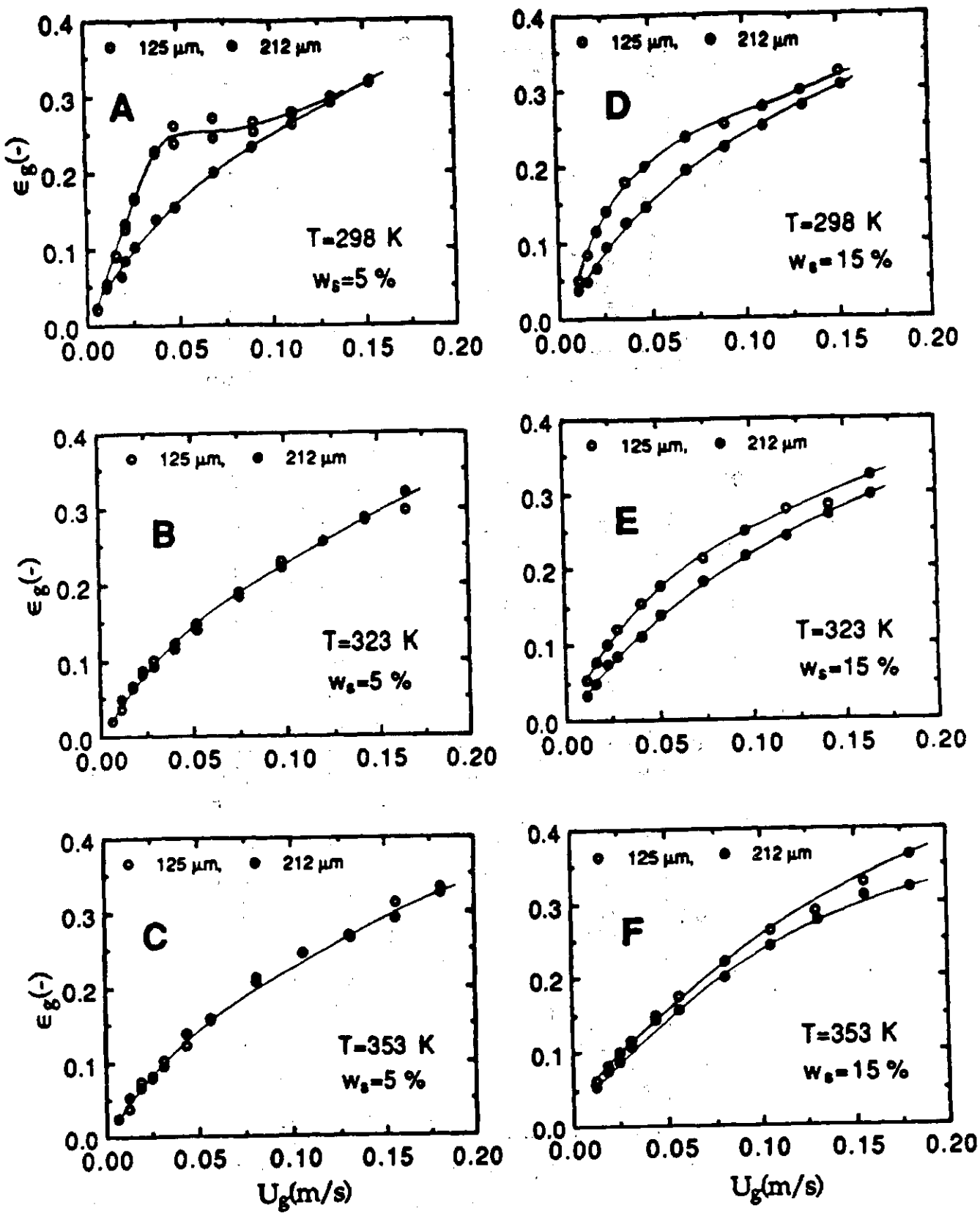

Fig. 4.56. Effect of particle diameter on air holdup at different temperatures for two slurry concentrations.

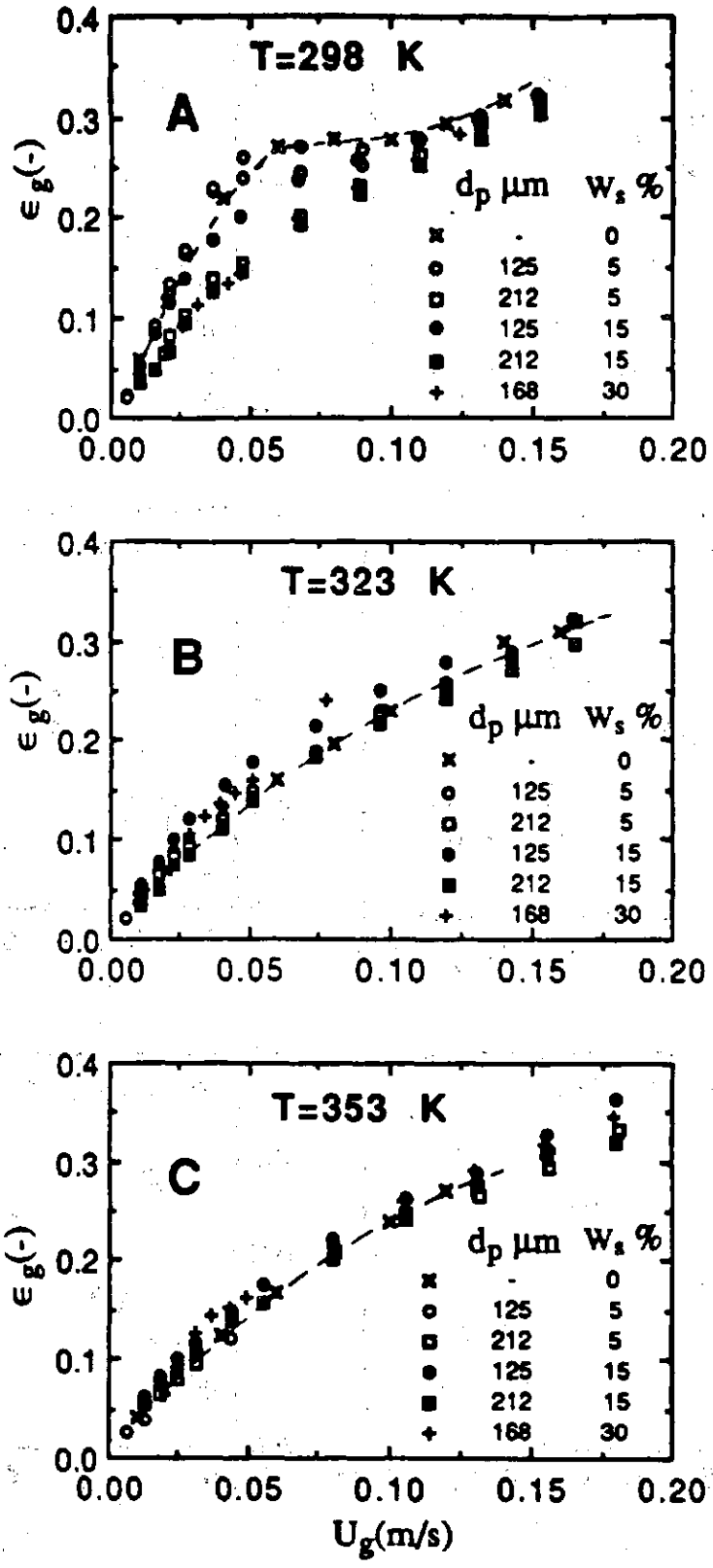

Fig. 4.57. Effect of slurry concentration on air holdup at different temperatures and slurry particle sizes.

temperature dependence for slurries of particle sizes equal to or greater than 168 μm, and for slurry concentrations greater than 15 weight percent. Fortunately, these are only the operating conditions likely to be met in practice.

The influence of particle diameter in the slurry on air holdup is explicitly shown in Fig. 4.56. An interesting trend is evident in these plots. For dilute slurries (about 5 weight percent) at ambient temperature (298K), the air holdup decreases with the increase in particle diameter. At higher temperatures, about (323K) and greater, this effect seems to fade away. On the other hand for relatively concentrated slurries (greater than 5 weight percent), the holdup decreases with increase in particle diameter over the entire range, 298 - 353K. Probably, this decrease in air holdup with increase in particle diameter appears to decrease with increase in temperature. In summary, the air holdup for dilute slurries (5 weight percent), the particle size effect is negligible above the ambient temperature while for concentrated slurries it will not be negligible except at higher temperatures.

The effect of slurry concentration for the data presented in Fig. 4.57 appears to be small in all cases. The values for the air-water system represented by a broken curve are smooth values of 4 sets of data points at each temperature. At ambient temperature, the effect is most pronounced for smallest particle size slurry and it appears to fade for slurries of larger particle size. At higher temperatures, the influence of slurry concentration on air holdup is reversed. The air holdup for smaller particle slurries, decreases with decrease in slurry concentration, while for larger particle slurries this change is negligible. In summary, the slurry concentration effect on slurries of larger particles is negligible at all temperatures but this effect may be considered for slurries of smaller particles.

Smoothed values of air holdup for these two systems are also reported in Table 4.23. In Fig. 4.52C, are shown the air holdup values averaged for slurries containing particles of average diameters 50 and 90 μm over the entire temperature range, 297 - 353K. Similar additional values for slurries containing particles greater than 100 μm will be useful.

Experiments have been conducted in 0.305 m bubble column equipped with a thirty-seven tube bundle for air-water-glass bead system for air holdup with

decreasing superficial air velocities at three temperatures (298, 323, and 353K) with the results reported in Fig. 4.53 - 4.55.

For slurries of 125 μm and 212 μm particles, two slurry concentrations have been examined, 5 and 15 weight percent. Figure 4.55 presents the single data set for the slurry of 168 μm particles taken for the slurry concentration of 30 weight percent. The holdup in all cases increases with increase in air velocity. The influence of temperature is relatively modest for a given slurry at a given air velocity. However, a small trend in the data suggests that this influence is relatively more for slurries of smaller particles and at smaller concentrations of solids in the slurry of same particle size. The temperature dependence is pronounced as the temperature is raised above the ambient (298K) but this dependence disappears as the temperature is raised (323 and 353K). For design purposes, it would appear to be appropriate to ignore the temperature dependence for slurries of particle sizes equal to or greater than 168 μm, and for slurry concentrations greater than 15 weight percent. Fortunately, these are only the operating conditions likely to be met in practice.

The influence of particle diameter in the slurry on air holdup is explicitly shown in Fig. 4.56. An interesting trend is evident in these plots. For dilute slurries (about 5 weight percent), at ambient temperature (298K), the air holdup decreases with the increase in particle diameter. At higher temperatures, about 323K and greater, this effect seems to fade away. On the other hand for relatively concentrated slurries (greater than 5 weight percent), the holdup decreases with increase in particle diameter over the entire range, 298-353K. Probably, this decrease in air holdup with increase in particle diameter appears to decrease with increase in temperature. In summary, the air holdup for dilute slurries (5 weight percent), the particle size effect is negligible except at higher temperatures.

The effect of slurry concentration for the data presented in Fig. 4.57 appears to be small in all cases smoothed air holdup data is given in Table 4.27. The values for the air-water system represented by a broken curve are smooth values of 4 sets of data points at each temperature. At ambient temperature, the effect is most pronounced for smallest particle size slurry and it appears to fade for slurries of larger particle size. At higher temperatures, the influence of slurry

Table 4.27. Smoothed air holdup values for air-water-glass bead system at different temperature levels. Column diameter: 0.305m, Internal: Thirty-seven tube bundle.

ϵ_g / U_g	d_p = 125 µm				d_p = 212 µm			d_p = 168 µm
	W_s = 5wt%		= 15wt%		= 5wt%		=15wt%	= 30wt%
	298K	323 & 353K	298K	323 & 353K	298K	323 & 353K	298, 323 & 353K	289, 323 & 353K
0.02	0.130	0.070	0.110	0.090	0.080	0.070	0.065	0.080
0.04	0.245	0.120	0.185	0.150	0.145	0.120	0.120	0.135
0.06	0.260	0.165	0.225	0.190	0.185	0.150	0.165	0.180
0.08	0.260	0.200	0.250	0.220	0.220	0.190	0.200	0.215
0.10	0.270	0.230	0.270	0.255	0.250	0.230	0.238	0.250
0.12	0.290	0.255	0.288	0.280	0.278	0.258	0.265	0.278
0.14	0.310	0.280	0.310	0.300	0.305	0.280	0.288	0.305
0.16	-	0.305	0.330	0.320	-	0.305	0.305	0.320
0.18	-	0.325	-	0.360	-	0.330	0.320	0.340

concentration on air holdup is reversed. The air holdup for smaller particle slurries decreases with decrease in slurry concentration, while for larger particle slurries this change is negligible. In summary, the slurry concentration effect on slurries of large particles is negligible at all temperatures but this effect may be considered for slurries of smaller particles.

4.5.6 Air-Water-Magnetite System

Air holdup data for the air-water-magnetite system as a function of air velocity at three temperatures are shown in Fig. 4.58. These data refer to slurries of 3 weight percent for 50 μm; 5 and 10 weight percent for 90 μm average diameter magnetite powders. In general, there is a good agreement between the holdup values referring to a particular temperature but for slurries of different concentrations and mean particle sizes. We have considered it appropriate to represent these values at each temperature with a single set of smoothed values. These averaged air holdup values are reported in Table 4.28. The air holdup values increase with increase in air velocity at each temperature but decrease with increase in temperature at a given air velocity. For comparison the air-water holdup data are also shown. The two sets of values are in good agreement with each other signifying that the presence of solids in a liquid does not appreciably influence the magnitude of gas holdup.

4.5.7 Nitrogen-Therminol-Magnetite System

The bubbling and foaming characteristics for the three-phase system are different than for the two-phase system. The nitrogen gas holdup values for the nitrogen-Therminol-magnetite system are shown plotted in Fig. 4.59 as a function of gas velocity for different temperatures. At 298K, the bubbling characteristics are the same for increasing and decreasing gas velocities. For gas velocities up to 30 mm/s, the bubbles formed are of about 4 - 5 mm in diameter above the distributor plate and these coalesce to form bubbles of about 10 mm diameter which rise in the central region of the column. Hardly any bubbles are seen in the outer peripheral region of the column. As the gas velocity is

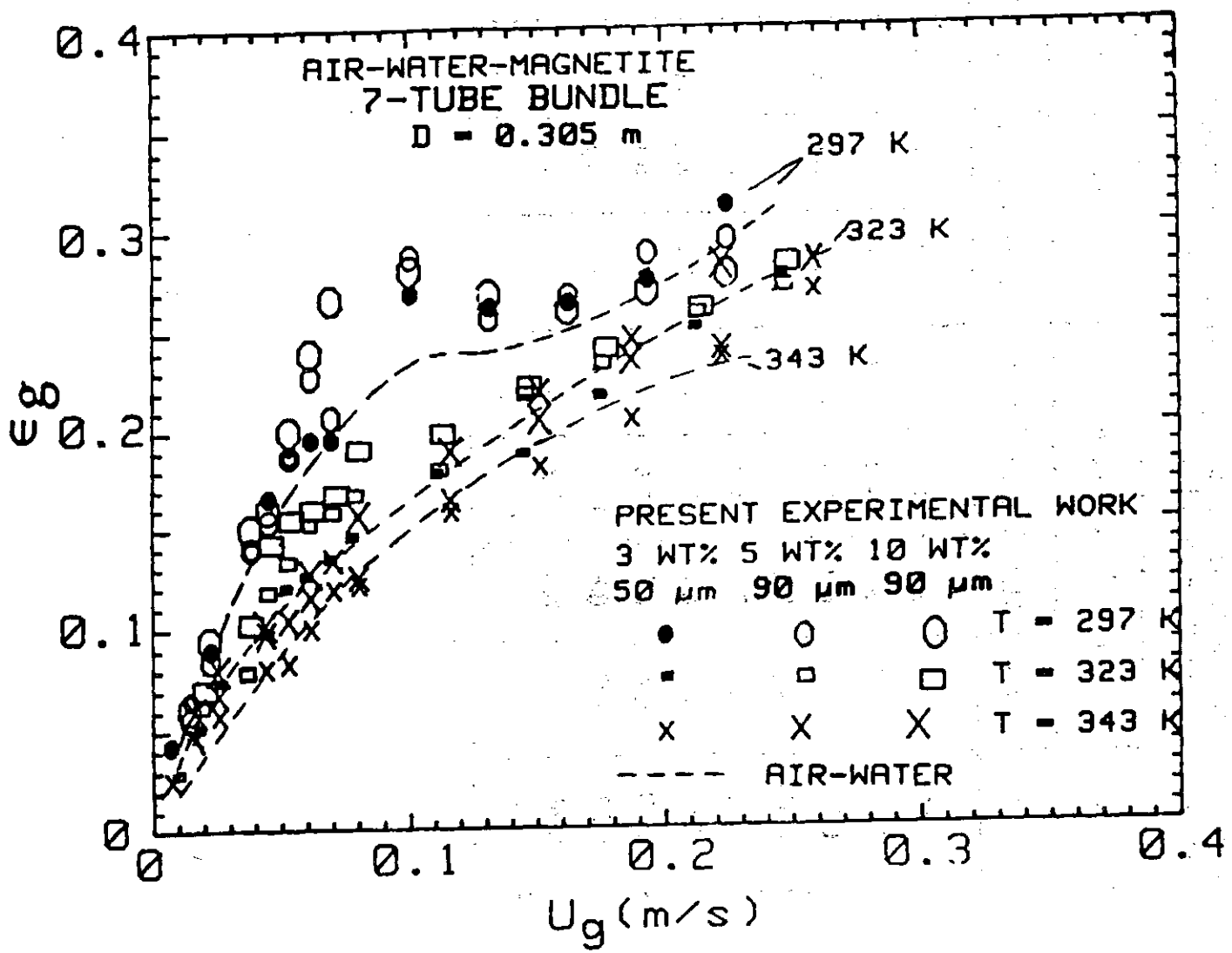

Fig. 4.58. Dependence of air holdup on air velocity, temperature, particles size and slurry concentration.

Table 4.28. Air holdup values smoothed over particle size and the solids concentration range for air-water-magnetite system at different temperature levels. Column diameter: 0.305 m, Internal: Seven-tube bundle. Particle diameters: 50 and 90 μm, Solids concentrations: 3, 5 and 10 wt%.

U_g	Air-Water System				Air-Water-Magetite System			
m/s	297K	313K	343K	353K	297K	323K	343K	353K
0.02	4.7	5.7	8.2	11.2	4.7	5.9	8.5	10.6
0.03	5.0	6.2	9.0	11.7	4.9	6.2	9.0	11.5
0.05	5.3	6.8	10.0	11.0	5.4	6.8	9.8	12.7
0.07	5.5	7.5	10.5	11.3	5.7	7.5	10.2	13.6
0.10	5.8	7.8	11.0	-	6.0	8.0	10.9	15.0
0.15	6.2	8.2	11.5	-	6.5	8.6	11.5	-
0.20	6.4	8.5	11.6	-	6.8	9.1	12.3	-
0.22	6.5	8.8	11.7	-	7.0	9.2	12.4	-
0.24	-	8.8	11.7	-	-	9.4	-	-
0.26	-	-	11.7	-	-	-	-	-

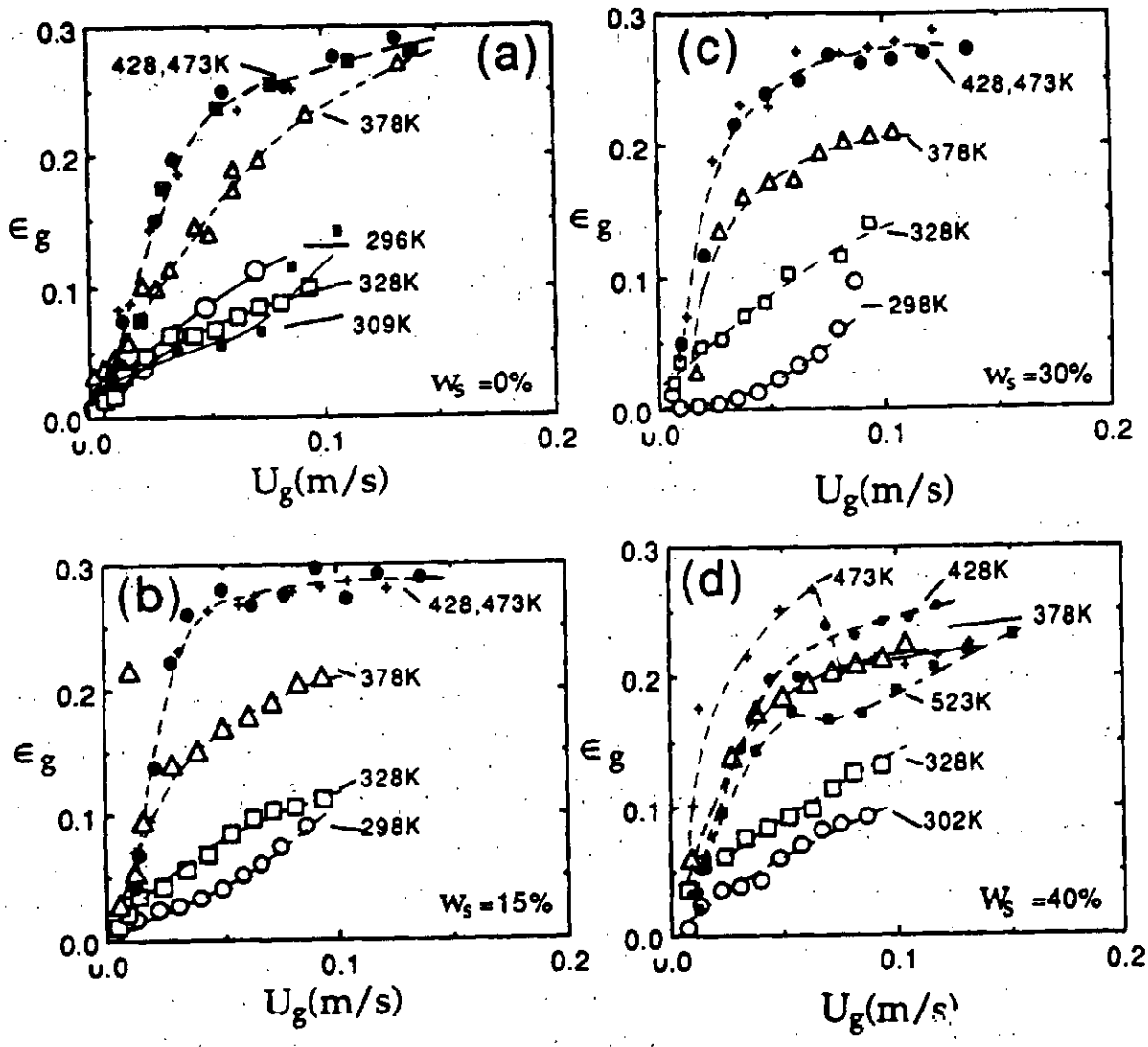

Fig. 4.59. Effect of temperature on nitrogen holdup at different solids concentrations in the slurry. 0 = 298K, □ =328K, △ =378K, • = 428K, + = 473K, ■ = 523K.

increased form 30 mm/s to 60 mm/s, the size of the coalesced bubbles increase up to 40 mm in diameter but tiny bubbles of about 1 mm diameter are also observed throughout the dispersion, and these remain trapped in the column for a longer period. As the gas velocity is further increased from 60 mm/ s to about 90 mm/s, the bubble size increases to about 60 - 70 mm; slugging is not observed as also the foam formation.

At 328K, no bubble coalescence is observed for gas velocities smaller than 60 mm/s. The bubbling characteristic is different than at 298K and bubbles of sizes varying between 2 to 5 mm rise up in the column, and circulation of these bubbles along with the liquid at higher velocities is observed. Tiny bubbles are not observed as at 25°C but the entire column is filled with bubbles of increasing sizes up to 20 - 30 mm, and these rise centrally in the column. No foaming is observed. At 378K, similar bubble behavior is observed except foam formation sets in and an average foam height of about 1 cm is observed at the top of the slurry column for gas velocities above 30 mm/s.

At higher temperatures (428, 473 and 523K) foam formation is observed whose intensity depends on slurry concentration, temperature, and how the gas velocity is approached i. e., whether in the increasing or in the decreasing mode. The nature of bubble dynamics on the other hand is the same over the entire temperature range. In this temperature range at about 0.5 m above the plate, 5 - 6 mm bubbles are formed at the distribution plate and split into smaller size bubbles, 2 -3 mm is size. These bubbles are distributed throughout the dispersion in the column. This behavior is observed for gas velocities up to about 30 mm/s, and the foam accumulation at the top of the dispersion in the column steadily increases up to 50 mm in height with increase in gas velocity in this range. For gas velocities in the range 30-80mm/s, the foam formation increases dramatically and its magnitude depends on the direction (increasing or decreasing) adopted to approach a certain value of the gas velocity. For increasing gas velocities up to about 80mm/s foam height up to 150mm is observed while the bubbling behavior remains the same as in the lower velocity range and foaming does not appreciably depend on the slurry concentration. For gas velocities in the decreasing mode, from a maximum value of 80mm/s to 30mm/s, the foam